

## The Crystal Structure of $\text{Nb}_8\text{W}_9\text{O}_{47}$

BY D. C. CRAIG AND N. C. STEPHENSON

*School of Chemistry, University of New South Wales, Australia*

(Received 9 September 1968 and in revised form 4 November 1968)

The crystal structure of the compound  $\text{Nb}_8\text{W}_9\text{O}_{47}$  has been determined from photographically recorded X-ray data. Fourier and least-squares methods were used to refine the structure which can be described either in terms of threefold or ninefold tetragonal tungsten-bronze subcell units. The observed splitting of certain X-ray reflexions requires that either the  $\text{Nb}_8\text{W}_9\text{O}_{47}$  phase is intergrown with a  $\text{Nb}_6\text{W}_8\text{O}_{39}$  phase, or that there is twinning of the threefold tetragonal tungsten-bronze subcell unit about the [130] axis. These yield essentially the same structure and it is probable that both twinning and intergrowth of phases occur in the one crystal. The 'single' crystal of  $\text{Nb}_8\text{W}_9\text{O}_{47}$  can be described as a continuous host matrix of corner sharing metal-oxygen polyhedra in which the metal atoms are average or (0.4 Nb + 0.6 W) atoms. Certain of the five-sided tunnels in this structure, which run parallel to the  $c$  axis, are filled with niobium and oxygen atoms so that the niobium atoms have pentagonal bipyramidal coordination. These filled tunnels are stacked in close-packed hexagonal array.

### Introduction

The compound  $\text{Nb}_8\text{W}_9\text{O}_{47}$ , or  $4\text{Nb}_2\text{O}_5 \cdot 9\text{WO}_3$ , was first described by Roth & Wadsley (1965) as a stable phase in the binary system  $\text{Nb}_2\text{O}_5:\text{WO}_3$ . These workers observed that powder diffraction data from this compound were very similar to those obtained from the tetragonal potassium tungsten-bronze (Magnéli, 1949) and consequently it was suggested that the structure of  $\text{Nb}_8\text{W}_9\text{O}_{47}$  is based upon a tetragonal tungsten-bronze subcell. It has since been shown (Stephenson, 1968) that a number of the stable phases in the region  $\text{Nb}_2\text{O}_5 \cdot \text{WO}_3:\text{WO}_3$  have structures based upon a tetragonal tungsten-bronze subcell; the differing unit-cells and symmetries associated with these various phases arise from the manner in which the five-membered rings, which become tunnels in three dimensions, are filled with metal and oxygen atoms.

The structure of a compound with the *ideal* formula  $\text{Nb}_8\text{W}_9\text{O}_{47}$  was first reported by Sleight & Magnéli (1964) and in more detail by Sleight (1966). The crystal structure was found to be made up of three tetragonal tungsten-bronze-like unit cells with four out of the twelve possible fivefold rings occupied by cations with oxygen atoms above and below, forming pentagonal bipyramidal coordination polyhedra. The fractional occupancies of the metal atomic sites were found to vary between 16 and 100% and the host lattice of corner sharing octahedra appeared to be discontinuous with a disordering of metal and oxygen atoms in the pentagonal tunnels. Sleight reported the *actual* composition of his crystal to be  $\text{Nb}_4\text{W}_6\text{O}_{28}$ , or  $2\text{Nb}_2\text{O}_5 \cdot 6\text{WO}_3$ , a considerable deviation from the stoichiometry expected for the ideal structure described by him.

We report below the structure of  $\text{Nb}_8\text{W}_9\text{O}_{47}$ , made from an  $\text{Nb}_2\text{O}_5:\text{WO}_3$  mixture in the molar ratio 4:9. There are no fractional occupancies of atomic sites and

niobium atoms are ordered in certain of the five-membered rings.

### Experimental

Crystals of  $\text{Nb}_8\text{W}_9\text{O}_{47}$  were prepared by Dr R. S. Roth, National Bureau of Standards, Washington, D.C., U.S.A. The compound is stable from at least 1150°C and well formed needles were produced when an intimate  $\text{Nb}_2\text{O}_5:\text{WO}_3$  mixture in the molar ratio 4:9 was heated in a sealed platinum tube at 1250°C for 100 hr and then quench-cooled.

A small crystal of length 0.02 cm and average cross sectional dimension of 0.004 cm was used to collect X-ray data. Zero layer precession photographs taken with Mo  $K\alpha$  radiation yielded cell dimensions which appeared to be in excellent agreement with those obtained by Roth (1967) from powder data, *i.e.*  $a = 36.69$ ,  $b = 36.57$ ,  $c = 3.945$  Å. The  $c$  axis of the orthorhombic cell is parallel to the needle axis of the crystal. The only systematic absences noted in the diffraction data occurred for reflexions  $h00$  with  $h = 2n + 1$  and  $0k0$  with  $k = 2n + 1$ . The space group is therefore  $P2_12_12$ .

Equi-inclination Weissenberg geometry, with Cu  $K\alpha$  radiation, was used to collect data about the  $c$  axis and intensities were estimated visually by multiple film techniques, a microscope eyepiece and a standard series of spots recorded in the usual manner. Data processing was effected on an IBM 360/50 computer with the use of programs written by D. C. Craig.

### Structure determination

A survey of the corrected intensities drew attention to a nearly identical distribution for zero and upper level reflexions. Also,  $hkl$  reflexions were particularly intense when both  $h$  and  $k = 3n$ , and it would seem that the structure is based upon the tetragonal tungsten-bronze

subcell, tripled along both the *a* and *b* directions, with all atoms lying close to the (001) and (002) planes and with the metal atoms in one of these planes.

The tetragonal tungsten-bronze structure (see Fig. 1), was deduced by Magnéli (1949) for the phase  $\text{K}_x\text{WO}_3$  ( $0.48 < x < 0.54$ ). It can be viewed as a two-dimensional network of corner-sharing octahedra which extends in a third direction, again by corner sharing. These networks form 3, 4 and 5-membered rings which become tunnels in three dimensions. The tunnels may be partially filled as in the various tungsten bronzes of the type  $A_x\text{WO}_3$  (Hägg & Magnéli, 1954) or they may be completely filled with cations as in  $\text{K}_6\text{Li}_4\text{Nb}_{10}\text{O}_{30}$  (Rubin, van Uitert & Levinstein, 1968) and in  $\text{Ba}_6\text{Ti}_2\text{Nb}_8\text{O}_{30}$  (Stephenson, 1965). In this latter instance the barium ions occupying the five-sided tunnels have tenfold coordination with oxygen atoms since the barium ions do not lie in the same plane as the octahedrally coordinated metal atoms. The five-sided tunnels may also be filled with metal and oxygen atoms to form a string of pentagonal bipyramids which share apices; in this case all the metal atoms lie in the same plane. Examples of this are  $\text{Mo}_{17}\text{O}_{47}$  (Kihlberg, 1963),  $\text{NaNb}_6\text{O}_{15}\text{F}$  and  $\text{NaNb}_6\text{O}_{15}\text{OH}$  (Andersson, 1965),  $\text{Nb}_{18}\text{W}_{16}\text{O}_{93}$ ,  $\text{Nb}_{18}\text{W}_{17}\text{O}_{96}$  and  $\text{Nb}_4\text{W}_7\text{O}_{31}$  (Stephenson, 1968).

There are 97 atoms in the asymmetric unit and well over 3000 reflexions on levels  $hk0-3$ . However, in view of the rather poor quality of these data (see also the *Discussion*), and the short length of the *c* axis, it was decided to solve the structure in projection by the use of  $hk0$  reflexions only. Details of puckering in the sheets of atoms running parallel to (001) are thereby lost but nevertheless the main features of the structure can be elucidated.

Ideal positions for the octahedrally coordinated metal atoms were evaluated from the previously tabulated atomic parameters for the tetragonal tungsten-bronze (Stephenson, 1968). Average form factors, equal to  $(\text{Nb} + \text{W})/2$ , based upon the relative numbers of metal atoms in the unit cell, were used in the calculation of structure factors. Successive cycles of structure factors and Fourier difference syntheses enabled the positions of all atoms to be determined although the oxygen atoms at  $z = \frac{1}{2}$  could not be distinguished from the metal atoms at  $z = 0$ , which they overlapped. Atomic form factors for oxygen and for niobium and tungsten were taken from Hoerni & Ibers (1954) and from Thomas & Umeda (1957) respectively. The zero oxidation state was assumed for each element and corrections for the real component of the anomalous dispersion of  $\text{Cu K}\alpha$  by tungsten and niobium were made with the  $\Delta f'$  values given by Dauben & Templeton (1955).

### Structure refinement

The structure of  $\text{Nb}_8\text{W}_9\text{O}_{47}$ , projected on to the (001) plane, is shown in Fig. 2. Twelve of the thirty-six pentagonal rings are filled with atoms and this is in agree-

ment with the number predicted from the 'compositional parallelogram' (Stephenson, 1968). This analytical procedure predicts that for a ninefold tetragonal tungsten-bronze subcell unit, a compound with composition  $\text{Nb}_8\text{W}_9\text{O}_{47}$  will have twelve metal atoms and twelve oxygen atoms in pentagonal rings. The peak heights of these atoms in electron density maps and also the values of occupancy factors in least-squares refinement cycles indicated that the metal atoms in pentagonal rings were niobium atoms. The remaining metal atoms in octahedral coordination had nearly identical peak heights and occupancy factors (taking the average atomic form factor).

The refinement of atomic parameters was carried out with the use of the full-matrix least-squares program of Busing, Martin & Levy, (1962). Niobium atomic form factors were used for the metal atoms in pentagonal rings and a composite form factor ( $0.4 \text{ Nb} + 0.6 \text{ W}$ ), based upon the relative numbers of remaining metal atoms, was used for atoms in octahedral coordination. Oxygen atoms, superimposed upon these metal atoms, were used in the structure factor calculations but their atomic parameters were not treated as variables in the least-squares refinement cycles. The thermal parameter of every oxygen atom was kept at a constant  $2.0 \text{ \AA}^2$  (based upon difference Fourier synthesis) during least-squares cycles owing to the limited storage capacity of the computer. The positional parameters *x* and *y*, and isotropic thermal parameters of the remaining atoms were allowed to vary. One final cycle was run in which the fractional occupancy factors of the metal atoms as well as the above parameters were allowed to vary. There were significant increases in the occupancy factors associated with atoms Me(3), Me(4) and Me(5), indicating that the tungsten atoms tend to prefer po-

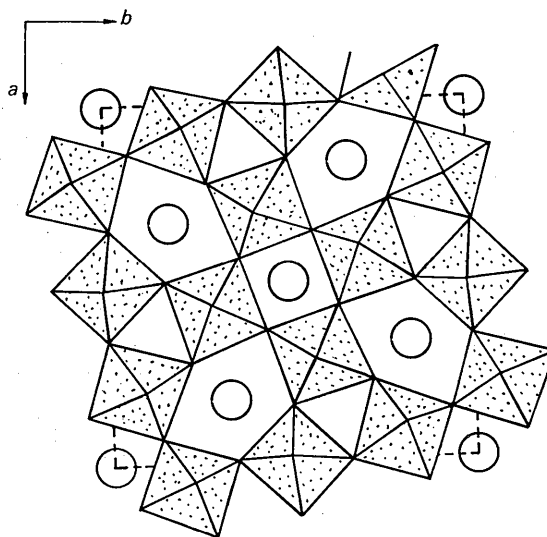


Fig. 1. The tetragonal tungsten-bronze structure viewed in projection along [001]. The four and five-membered rings may be occupied by metal atoms, shown as open circles.

sitions adjacent to the tunnels occupied by niobium atoms.

The weighting scheme used was that of Cruickshank (1965), viz.  $w = 1/(a + |F_o| - c|F_o|^2)$  where  $a$  and  $c$  are equal to  $2 F_{\min}$  and  $2/F_{\max}$  respectively. The 'accidentally absent' reflexions which were too weak to be observed were given an estimated intensity of  $I_{\min}/4$  and were included in the least-squares refinement with constant weights such that their average  $w\Delta^2$  value was the same as for the 'observed' reflexions. These data are quite extensive and consist mainly of  $hk0$  reflexions where  $h \neq 3n$ .

The final positional coordinates and isotropic temperature factors for the crystallographically independent atoms, together with estimated standard deviations, are given in Table 1. A list of observed and calculated structure factors is given in Table 2 and the reliability index  $R$  for all observed data is 0.13.

Table 1. Atomic parameters for  $Nb_8W_9O_{47}$  based upon a ninefold tetragonal tungsten bronze subcell unit

Standard deviations are given in brackets and refer to the last two places of the preceding number. All atoms listed in the above table have  $z/c = 0$ . Me atoms are (0.4 Nb + 0.6 W) atoms.  $P$  represents one niobium atom. There are also oxygen atoms (not listed) superimposed on Me and  $P$  atoms, each with a  $z/c$  coordinate of 0.500 and thermal parameter,  $B$ , equal to  $2.00 \text{ \AA}^2$ .

	$x/a$	$y/b$	$B$
Me(1)	0.0000	0.50000	6.28 (74) $\text{\AA}^2$
Me(2)	0.16581 (26)	-0.00124 (23)	0.22 (23)
Me(3)	0.00516 (33)	0.17202 (29)	2.43 (33)
Me(4)	0.17151 (26)	0.32518 (20)	-0.56 (22)
Me(5)	0.33765 (31)	0.17135 (26)	1.35 (29)
Me(6)	0.02407 (35)	0.07053 (29)	2.55 (34)
Me(7)	0.30518 (35)	0.26637 (30)	2.59 (34)
Me(8)	0.07088 (30)	0.30627 (25)	1.25 (28)
Me(9)	0.26589 (32)	0.02208 (28)	2.26 (33)
Me(10)	0.14154 (34)	0.23245 (30)	2.60 (33)
Me(11)	0.19314 (34)	0.09685 (27)	2.06 (33)

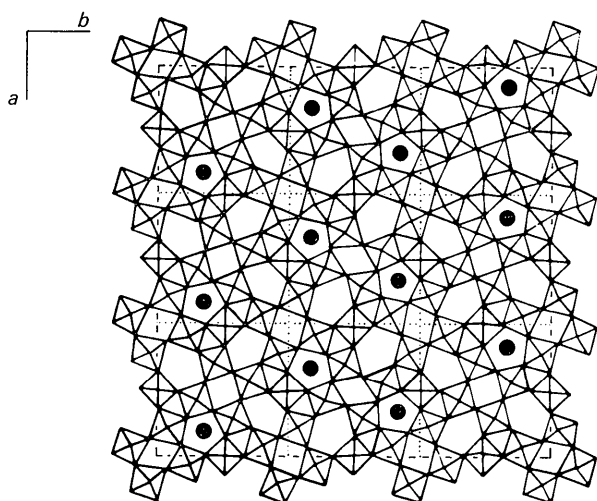


Fig. 2. The structure of  $Nb_8W_9O_{47}$  projected on to the (001) plane. Each full circle represents a niobium atom at  $z=0$  together with a superimposed oxygen atom at  $z=\frac{1}{2}$ . The metal atom has sevenfold coordination.

Table 1 (cont.)

	$x/a$	$y/b$	$B$
Me(12)	0.23555 (31)	0.19346 (26)	1.78 (30)
Me(13)	0.09661 (35)	0.14115 (30)	2.65 (34)
Me(14)	0.35761 (36)	0.06901 (31)	3.25 (36)
Me(15)	0.43146 (34)	0.13829 (30)	2.79 (34)
Me(16)	0.40348 (32)	0.30921 (27)	1.88 (31)
Me(17)	0.47480 (34)	0.23213 (29)	2.23 (32)
Me(18)	0.02267 (32)	0.40310 (26)	1.69 (30)
Me(19)	0.09750 (28)	0.47886 (23)	0.60 (25)
Me(20)	0.26590 (32)	0.36137 (27)	1.80 (30)
Me(21)	0.19221 (34)	0.42840 (28)	2.46 (33)
Me(22)	0.35577 (30)	0.40220 (24)	1.00 (28)
Me(23)	0.43155 (36)	0.47767 (32)	3.35 (37)
$P(1)$	0.10962 (35)	0.38848 (26)	-0.89 (28)
$P(2)$	0.27607 (52)	0.10963 (44)	3.16 (51)
$P(3)$	0.44743 (54)	0.38962 (47)	3.45 (65)
O(1)	0.0373 (27)	0.0185 (23)	
O(2)	0.0814 (27)	0.0886 (23)	
O(3)	0.0493 (27)	0.1672 (24)	
O(4)	0.1114 (27)	0.0055 (25)	
O(5)	0.1615 (26)	0.1156 (23)	
O(6)	0.1710 (27)	0.0518 (23)	
O(7)	0.2175 (26)	-0.0041 (24)	
O(8)	0.2385 (27)	0.0647 (23)	
O(9)	0.2358 (25)	0.1424 (23)	
O(10)	0.2985 (27)	0.0558 (23)	
O(11)	0.3696 (26)	0.0237 (24)	
O(12)	0.3273 (28)	0.1239 (23)	
O(13)	0.3017 (26)	0.1902 (23)	
O(14)	0.4072 (27)	0.0956 (23)	
O(15)	0.4808 (27)	0.1168 (23)	
O(16)	0.4969 (28)	0.0507 (23)	
O(17)	0.4534 (27)	0.0007 (24)	
O(18)	0.4467 (26)	0.1898 (23)	
O(19)	0.3932 (26)	0.1747 (24)	
O(20)	0.4362 (26)	0.2648 (24)	
O(21)	0.0037 (27)	0.2138 (23)	
O(22)	0.4562 (27)	0.3329 (24)	
O(23)	0.5002 (28)	0.3812 (23)	
O(24)	0.4661 (27)	0.4485 (23)	
O(25)	0.3994 (26)	0.4249 (24)	
O(26)	0.3825 (25)	0.3631 (24)	
O(27)	0.3569 (26)	0.2886 (23)	
O(28)	0.3370 (26)	0.2261 (24)	
O(29)	0.2671 (26)	0.2442 (23)	
O(30)	0.2834 (27)	0.3174 (24)	
O(31)	0.3164 (26)	0.3869 (23)	
O(32)	0.3361 (27)	0.4513 (24)	
O(33)	0.2079 (26)	0.4808 (23)	
O(34)	0.2410 (27)	0.3999 (23)	
O(35)	0.2152 (26)	0.3394 (23)	
O(36)	0.1758 (27)	0.2798 (24)	
O(37)	0.1943 (27)	0.2063 (23)	
O(38)	0.1188 (26)	0.1936 (24)	
O(39)	0.1028 (27)	0.2604 (23)	
O(40)	0.1207 (27)	0.3372 (24)	
O(41)	0.1656 (28)	0.3875 (23)	
O(42)	0.1339 (27)	0.4409 (23)	
O(43)	0.0686 (27)	0.4265 (24)	
O(44)	0.0626 (25)	0.3615 (23)	
O(45)	0.0207 (27)	0.2892 (23)	

The unit-cell dimensions and positional parameters listed in Table 1 were used to derive the interatomic distances listed in Table 3 and the bond angles listed in Table 4. The standard errors in these values were computed from the variance-covariance matrix obtained in the final least-squares refinement and the unit-cell errors by the use of the ORFFE program of Busing, Martin & Levy (1964).

Table 2. A list of absolute values of observed and calculated structure factors

The columns read, from left to right,  $hkl$  [ $F(\text{obs})$ ] and [ $F(\text{calc})$ ]. Unobserved reflexions are prefixed by the letter U.

0	4	0	569	445	9	15	0	844	783	19	6	0	165	36	U	3	27	0	72	111	U	10	8	0	43	62	U	17	4	0	52	37
0	4	0	433	230	9	18	0	2151	1826	19	7	0	117	59	U	3	32	0	78	187	U	10	9	0	44	40	U	17	5	0	53	67
0	8	0	296	300	9	20	0	124	826	19	9	0	186	121	U	3	37	0	76	73	U	10	10	0	46	40	U	17	6	0	52	47
0	10	0	1172	1094	6	21	0	313	292	19	24	0	156	112	U	3	38	0	74	57	U	10	13	0	50	30	U	17	8	0	45	38
0	12	0	1080	905	6	22	0	635	670	20	3	0	163	70	U	3	41	0	75	45	U	10	14	0	52	60	U	17	9	0	46	72
0	14	0	317	307	9	24	0	1275	1265	20	3	0	233	127	U	3	42	0	61	117	U	10	15	0	53	66	U	17	10	0	57	46
0	16	0	488	474	10	25	0	201	193	20	6	0	119	130	U	4	1	0	23	7	U	10	16	0	55	33	U	17	11	0	58	75
0	20	0	464	338	10	26	0	303	328	20	7	0	170	95	U	4	2	0	24	5	U	10	17	0	57	68	U	17	12	0	59	44
0	22	0	905	240	9	29	0	377	321	20	15	0	136	166	U	4	3	0	25	12	U	10	19	0	61	34	U	17	13	0	60	29
0	24	0	315	336	9	33	0	315	336	21	1	0	120	118	U	4	4	0	27	21	U	10	20	0	62	65	U	17	14	0	62	53
0	28	0	970	969	9	37	0	364	304	21	3	0	2395	2312	U	4	7	0	33	3	U	10	23	0	66	85	U	17	16	0	66	65
0	30	0	1172	1094	9	39	0	394	280	21	4	0	421	475	U	4	8	0	35	36	U	10	24	0	70	61	U	17	17	0	69	48
0	32	0	1080	905	9	39	0	480	438	21	5	0	122	139	U	4	10	0	39	17	U	10	25	0	71	58	U	17	18	0	70	45
0	34	0	317	307	9	41	0	124	186	21	7	0	176	256	U	4	11	0	41	22	U	10	26	0	73	43	U	17	19	0	69	48
0	36	0	488	474	10	43	0	507	507	21	8	0	437	441	U	4	13	0	44	1	U	10	28	0	76	35	U	17	20	0	70	48
0	40	0	464	338	10	46	0	76	82	21	8	0	312	280	U	4	14	0	46	29	U	10	29	0	78	108	U	17	21	0	70	45
0	42	0	905	240	10	48	0	98	105	21	10	0	517	592	U	4	16	0	50	57	U	10	30	0	80	57	U	17	22	0	71	71
0	44	0	1157	1261	10	51	0	317	114	21	12	0	326	313	U	4	17	0	52	44	U	10	31	0	82	41	U	17	23	0	73	80
0	46	0	140	240	10	53	0	118	109	21	13	0	468	487	U	4	19	0	56	22	U	10	32	0	84	61	U	17	24	0	74	129
0	48	0	147	203	10	27	0	150	139	21	15	0	883	851	U	4	20	0	58	33	U	10	33	0	86	33	U	17	25	0	75	139
0	50	0	970	969	11	3	0	163	138	21	21	0	1100	1050	U	4	22	0	63	22	U	10	34	0	88	22	U	17	26	0	76	165
0	52	0	598	518	11	6	0	209	199	21	21	0	432	489	U	4	23	0	65	27	U	10	35	0	90	66	U	17	27	0	77	187
0	54	0	310	302	11	12	0	142	186	21	23	0	220	148	U	4	25	0	68	29	U	10	36	0	92	29	U	17	28	0	77	48
0	56	0	148	148	11	18	0	170	76	21	24	0	362	549	U	4	26	0	70	70	U	10	37	0	94	42	U	17	29	0	78	73
0	58	0	277	81	11	24	0	200	115	21	25	0	315	313	U	4	27	0	72	72	U	10	38	0	96	34	U	17	30	0	79	104
0	60	0	966	792	12	0	0	1025	980	21	27	0	626	296	U	4	28	0	74	85	U	10	39	0	98	29	U	17	31	0	80	134
0	62	0	537	203	12	1	0	486	516	21	28	0	155	227	U	4	29	0	75	63	U	10	40	0	100	47	U	17	32	0	81	164
0	64	0	282	353	12	3	0	2294	2404	21	30	0	153	166	U	5	2	0	26	43	U	10	41	0	102	39	U	17	33	0	82	194
0	66	0	104	7	12	4	0	171	92	21	30	0	153	166	U	5	2	0	26	43	U	10	42	0	104	31	U	17	34	0	83	224
0	68	0	245	67	12	6	0	289	156	21	31	0	324	402	U	5	3	0	27	38	U	10	43	0	106	23	U	17	35	0	84	254
1	12	0	289	89	12	6	0	1521	1563	21	35	0	422	277	U	5	4	0	29	38	U	10	44	0	108	15	U	17	36	0	85	284
1	18	0	305	126	12	7	0	222	203	21	36	0	312	233	U	5	5	0	31	45	U	10	45	0	110	7	U	17	37	0	86	314
2	15	0	272	87	12	9	0	270	320	21	39	0	324	365	U	5	6	0	32	39	U	10	46	0	112	1	U	17	38	0	87	344
2	23	0	223	261	12	10	0	196	185	22	0	0	124	84	U	5	8	0	36	30	U	10	47	0	114	5	U	17	39	0	88	374
3	3	0	380	227	12	12	0	292	240	22	6	0	255	131	U	5	11	0	41	33	U	10	48	0	116	9	U	17	40	0	89	404
3	4	0	231	219	12	13	0	673	613	22	12	0	193	65	U	5	13	0	45	68	U	10	49	0	118	13	U	17	41	0	90	434
3	8	0	336	295	12	15	0	813	850	22	21	0	218	101	U	5	15	0	49	132	U	10	50	0	120	17	U	17	42	0	91	464
3	8	0	2123	1995	12	16	0	434	384	22	24	0	157	125	U	5	16	0	51	32	U	10	51	0	122	21	U	17	43	0	92	494
3	12	0	2474	2390	12	18	0	173	162	22	24	0	158	101	U	5	18	0	55	8	U	10	52	0	124	25	U	17	44	0	93	524
3	12	0	2474	2390	12	19	0	357	322	24	0	0	1256	1140	U	5	19	0	57	88	U	10	53	0	126	29	U	17	45	0	94	554
3	18	0	357	344	12	19	0	357	344	24	6	0	1116	1063	U	5	22	0	63	44	U	10	54	0	128	33	U	17	46	0	95	584
3	18	0	469	403	12	21	0	377	352	24	4	0	378	302	U	5	21	0	61	66	U	10	55	0	130	37	U	17	47	0	96	614
3	18	0	308	364	12	22	0	387	406	24	6	0	346	308	U	5	22	0	63	44	U	10	56	0	132	41	U	17	48	0	97	644
3	18	0	315	251	12	24	0	387	270	24	6	0	346	308	U	5	22	0	63	44	U	10	57	0	134	45	U	17	49	0	98	674
3	20	0	549	485	12	25	0	293	283	24	8	0	275	222	U	5	24	0	67	74	U	10	58	0	136	49	U	17	50	0	99	704
3	20	0	2072	2140	12	25	0	366	360	24	8	0	1257	1278	U	5	25	0	69	121	U	10	59	0	138	53	U	17	51	0	100	734
3	22	0	560	575	12	27	0	1656	1441	24	10	0	257	1278	U	5	26	0	71	71	U	10	60	0	140	57	U	17	52	0	101	764
3	24	0	533	520	12	28	0	154	186	24	11	0	441	441	U	5	27	0	72	104	U	10	61	0	142	61	U	17	53	0	102	794
3	24	0	274	288	12	28	0	220	238	24	12	0	351	301	U	5	28	0	74	43	U	10	62	0	144	65	U	17	54	0	103	824
3	24	0	148	174	12	31	0	223	204	24	13	0	145	123	U	5	29	0	75	45	U	10	63	0	146	69	U	17	55	0	104	854
3	29	0	213	223	12	33	0	157	123	24	15	0	419	495	U	5	30	0	76	47	U	10	64	0	148	73	U	17	56	0	105	884
3	30	0	658	732	12	34	0	152	154	24	16	0	609	284	U	5	31	0	78	32	U	10	65	0	150	77	U	17	57	0	106	914
3	30	0	711	779	12	35	0	152	154	24	16	0	609																			

Table 3. Selected interatomic distances (Å)  
in the compound  $\text{Nb}_8\text{W}_9\text{O}_{47}$

The superscripts denote the following symmetry transformations of the parameters of Table 1:

No	superscript	x	y	z
1		$\frac{1}{2} - x$	$\frac{1}{2} + y$	z
2		$x - \frac{1}{2}$	$\frac{1}{2} - y$	z
3		$\frac{1}{2} - x$	$y - \frac{1}{2}$	z
4		$\frac{1}{2} + x$	$\frac{1}{2} - y$	z

Me(1)—O(16) <sup>1</sup>	1.88 (09)
—O(17) <sup>1</sup>	1.69 (11)
—O(16) <sup>2</sup>	1.88 (09)
—O(17) <sup>2</sup>	1.69 (11)
Me(2)—O(4)	2.02 (11)
—O(6)	1.96 (09)
—O(7)	1.91 (10)
—O(32) <sup>3</sup>	1.72 (09)
Me(3)—O(3)	1.61 (11)
—O(21)	1.54 (09)
—O(22) <sup>2</sup>	1.84 (11)
—O(23) <sup>2</sup>	1.97 (09)
Me(4)—O(35)	1.67 (10)
—O(36)	1.66 (09)
—O(40)	1.92 (10)
—O(41)	2.33 (09)
Me(5)—O(12)	1.78 (09)
—O(13)	1.75 (10)
—O(28)	2.00 (09)
—O(19)	2.06 (10)
Me(6)—O(1)	2.03 (09)
—O(2)	2.19 (10)
—O(23) <sup>2</sup>	1.92 (09)
—O(24) <sup>2</sup>	2.22 (10)
Me(7)—O(27)	2.03 (10)
—O(28)	1.88 (10)
—O(29)	1.61 (10)
—O(30)	2.02 (09)
Me(8)—O(39)	2.06 (09)
—O(40)	2.13 (10)
—O(44)	2.07 (09)
—O(45)	1.92 (10)
Me(9)—O(7)	1.98 (10)
—O(8)	1.87 (09)
—O(10)	1.74 (10)
—O(33) <sup>3</sup>	1.83 (09)
Me(10)—O(36)	2.18 (09)
—O(37)	2.18 (10)
—O(38)	1.64 (09)
—O(39)	1.73 (10)
Me(11)—O(5)	1.33 (10)
—O(6)	1.86 (10)
—O(8)	2.02 (10)
—O(9)	2.29 (09)
Me(12)—O(9)	1.87 (09)
—O(13)	2.12 (10)
—O(29)	2.20 (09)
—O(37)	1.57 (10)
Me(13)—O(2)	1.99 (09)
—O(3)	1.99 (11)
—O(38)	2.10 (09)
—O(5)	2.57 (10)
Me(14)—O(12)	2.32 (09)
—O(10)	2.21 (11)
—O(11)	1.70 (09)
—O(14)	2.03 (10)
Me(15)—O(14)	1.81 (09)
—O(15)	1.94 (10)
—O(18)	1.96 (09)
—O(19)	1.92 (10)
Me(16)—O(20)	1.98 (09)
—O(22)	2.08 (11)

Table 3 (cont.)

—O(26)	2.14 (09)
—O(27)	1.89 (10)
Me(17)—O(18)	1.86 (09)
—O(20)	1.88 (10)
—O(21) <sup>4</sup>	2.23 (09)
—O(45) <sup>4</sup>	1.89 (10)
Me(18)—O(44)	2.08 (09)
—O(43)	1.85 (10)
—O(16) <sup>2</sup>	1.92 (09)
—O(15) <sup>2</sup>	1.73 (10)
Me(19)—O(42)	1.89 (10)
—O(43)	2.22 (09)
—O(17) <sup>1</sup>	2.04 (11)
—O(11) <sup>1</sup>	2.05 (10)
Me(20)—O(30)	1.75 (09)
—O(31)	2.17 (10)
—O(34)	1.67 (09)
—O(35)	2.04 (10)
Me(21)—O(33)	2.00 (09)
—O(34)	2.08 (10)
—O(41)	1.73 (10)
—O(42)	2.26 (11)
Me(22)—O(25)	1.78 (10)
—O(26)	1.70 (09)
—O(31)	1.48 (10)
—O(32)	1.94 (09)
Me(23)—O(24)	1.68 (10)
—O(25)	2.29 (09)
—O(4) <sup>1</sup>	1.84 (10)
—O(1) <sup>1</sup>	1.85 (10)
P(1)—O(40)	1.94 (09)
—O(41)	2.07 (11)
—O(42)	2.07 (09)
—O(43)	2.07 (10)
—O(44)	2.00 (10)
P(2)—O(8)	2.18 (10)
—O(9)	1.92 (10)
—O(13)	2.36 (09)
—O(12)	1.88 (10)
—O(10)	2.12 (09)
P(3)—O(22)	2.13 (09)
—O(23)	2.00 (11)
—O(24)	2.24 (09)
—O(25)	2.16 (10)
—O(26)	2.56 (10)
O(16) <sup>1</sup> —O(17) <sup>1</sup>	2.46 (14)
O(17) <sup>1</sup> —O(16) <sup>2</sup>	2.59 (14)
O(16) <sup>2</sup> —O(17) <sup>2</sup>	2.46 (14)
O(17) <sup>2</sup> —O(16) <sup>1</sup>	2.59 (14)
O(4)—O(6)	2.73 (15)
O(6)—O(7)	2.74 (14)
O(7)—O(32) <sup>3</sup>	2.62 (14)
O(32) <sup>3</sup> —O(4)	2.67 (14)
O(3)—O(21)	2.39 (14)
O(21)—O(22) <sup>2</sup>	2.45 (14)
O(22) <sup>2</sup> —O(23) <sup>2</sup>	2.47 (14)
O(23) <sup>2</sup> —O(3)	2.52 (14)
O(35)—O(36)	2.55 (13)
O(36)—O(40)	2.94 (14)
O(40)—O(41)	2.55 (14)
O(41)—O(35)	2.55 (14)
O(12)—O(13)	2.21 (13)
O(13)—O(28)	2.61 (13)
O(28)—O(19)	2.81 (14)
O(19)—O(12)	3.10 (14)
O(1)—O(2)	3.09 (14)
O(2)—O(23) <sup>2</sup>	3.12 (14)
O(23) <sup>2</sup> —O(24) <sup>2</sup>	2.73 (14)
O(24) <sup>2</sup> —O(1)	2.87 (14)
O(27)—O(28)	2.40 (13)
O(28)—O(29)	2.65 (14)
O(29)—O(30)	2.84 (15)

Table 3 (cont.)

O(30)—O(27)	2.84 (15)
O(39)—O(40)	2.83 (13)
O(40)—O(44)	2.34 (14)
O(44)—O(45)	3.06 (13)
O(45)—O(39)	3.20 (15)
O(7)—O(8)	2.58 (13)
O(8)—O(10)	2.29 (15)
O(10)—O(33) <sup>2</sup>	2.72 (13)
O(33) <sup>2</sup> —O(7)	2.88 (14)
O(36)—O(37)	2.81 (13)
O(37)—O(38)	2.82 (14)
O(38)—O(39)	2.50 (13)
O(39)—O(36)	2.78 (14)
O(5)—O(6)	2.31 (13)
O(6)—O(8)	2.57 (15)
O(8)—O(9)	2.85 (13)
O(9)—O(5)	2.90 (14)
O(13)—O(29)	2.76 (13)
O(29)—O(37)	3.03 (14)
O(37)—O(9)	2.76 (13)
O(2)—O(3)	3.09 (13)
O(3)—O(38)	2.72 (15)
O(38)—O(5)	3.29 (13)
O(5)—O(2)	3.11 (15)
O(12)—O(10)	2.69 (13)
O(10)—O(11)	2.84 (15)
O(11)—O(14)	2.93 (14)
O(14)—O(12)	3.14 (14)
O(14)—O(15)	2.80 (15)
O(15)—O(18)	2.94 (13)
O(19)—O(14)	2.92 (13)
O(20)—O(22)	2.53 (13)
O(22)—O(26)	2.92 (14)
O(26)—O(27)	2.90 (13)
O(27)—O(20)	3.04 (15)
O(18)—O(20)	2.81 (13)
O(20)—O(21)	2.60 (14)
O(21)—O(45)	2.83 (13)
O(45)—O(18)	2.85 (15)
O(44)—O(43)	2.34 (13)
O(43)—O(16) <sup>2</sup>	2.73 (15)
O(16) <sup>2</sup> —O(15) <sup>2</sup>	2.47 (13)
O(15) <sup>2</sup> —O(44)	3.11 (14)
O(42)—O(43)	2.41 (15)
O(43)—O(17)	2.81 (14)
O(17)—O(11)	3.21 (15)
O(11)—O(41)	3.06 (13)
O(30)—O(31)	2.89 (13)
O(31)—O(34)	2.85 (15)
O(34)—O(35)	2.44 (13)
O(35)—O(30)	2.67 (14)
O(33)—O(34)	3.25 (13)
O(34)—O(41)	2.78 (14)
O(41)—O(42)	2.28 (14)
O(42)—O(33)	3.07 (14)
O(25)—O(26)	2.31 (13)
O(26)—O(31)	2.53 (14)
O(31)—O(32)	2.42 (13)
O(32)—O(15)	2.45 (14)
O(24)—O(25)	2.62 (15)
O(25)—O(4) <sup>1</sup>	2.95 (14)
O(4) <sup>1</sup> —O(1) <sup>1</sup>	2.78 (14)
O(1) <sup>1</sup> —O(24)	2.52 (13)
O(40)—O(41)	2.55 (14)
O(41)—O(42)	2.28 (14)
O(42)—O(43)	2.41 (15)
O(43)—O(44)	2.34 (13)
O(44)—O(40)	2.34 (14)
O(8)—O(9)	2.85 (13)
O(9)—O(13)	2.26 (14)
O(13)—O(12)	2.59 (13)
O(12)—O(10)	2.70 (13)

Table 3 (cont.)

O(10)—O(8)	2.29 (15)
O(22)—O(23)	2.47 (14)
O(23)—O(24)	2.73 (14)
O(24)—O(25)	2.62 (15)
O(25)—O(26)	2.31 (13)
O(26)—O(22)	2.92 (15)

Table 4. Selected interatomic angles (°) in the compound Nb<sub>8</sub>W<sub>9</sub>O<sub>47</sub>

The symmetry transformations, denoted by superscripts, are the same as in Table 3. Standard deviations are given in parentheses.

O(16) <sup>1</sup> —Me(1)—O(17) <sup>1</sup>	87.0 (4.6)
O(17) <sup>1</sup> —Me(1)—O(16) <sup>2</sup>	93.0 (4.6)
O(16) <sup>2</sup> —Me(1)—O(17) <sup>2</sup>	87.0 (4.6)
O(17) <sup>2</sup> —Me(1)—O(16) <sup>1</sup>	93.0 (4.6)
O(16) <sup>1</sup> —O(17) <sup>1</sup> —O(16) <sup>2</sup>	96.2 (4.6)
O(17) <sup>1</sup> —O(16) <sup>2</sup> —O(17) <sup>2</sup>	83.8 (4.6)
O(16) <sup>2</sup> —O(17) <sup>2</sup> —O(16) <sup>1</sup>	96.2 (4.6)
O(17) <sup>2</sup> —O(16) <sup>1</sup> —O(17) <sup>1</sup>	83.8 (4.6)
O(4)—Me(2)—O(6)	86.8 (4.3)
O(6)—Me(2)—O(7)	90.2 (4.2)
O(7)—Me(2)—O(32) <sup>3</sup>	92.1 (4.4)
O(32) <sup>3</sup> —Me(2)—O(4)	90.9 (4.4)
O(4)—O(6)—O(7)	91.8 (3.9)
O(6)—O(7)—O(32) <sup>3</sup>	86.6 (4.0)
O(7)—O(32) <sup>3</sup> —O(4)	95.9 (4.1)
O(32) <sup>3</sup> —O(4)—O(6)	85.8 (4.1)
O(3)—Me(3)—O(21)	98.4 (5.1)
O(21)—Me(3)—O(22) <sup>2</sup>	92.2 (4.9)
O(22) <sup>2</sup> —Me(3)—O(23) <sup>2</sup>	80.6 (4.3)
O(23) <sup>2</sup> —Me(3)—O(3)	88.8 (4.6)
O(3)—O(21)—O(22) <sup>2</sup>	90.7 (4.5)
O(21)—O(22) <sup>2</sup> —O(23) <sup>2</sup>	91.1 (4.8)
O(22) <sup>2</sup> —O(23) <sup>2</sup> —O(3)	87.0 (4.4)
O(26) <sup>2</sup> —O(3)—O(21)	91.2 (4.7)
O(35)—Me(4)—O(36)	100.2 (4.6)
O(36)—Me(4)—O(40)	109.7 (4.4)
O(40)—Me(4)—O(41)	72.9 (3.9)
O(41)—Me(4)—O(35)	77.2 (4.2)
O(35)—O(36)—O(40)	77.9 (3.8)
O(36)—O(40)—O(41)	93.2 (4.5)
O(40)—O(41)—O(35)	85.8 (4.2)
O(41)—O(35)—O(36)	103.0 (4.8)
O(12)—Me(5)—O(13)	77.0 (4.8)
O(13)—Me(5)—O(28)	88.0 (4.4)
O(28)—Me(5)—O(19)	87.7 (3.9)
O(19)—Me(5)—O(12)	107.3 (4.2)
O(12)—O(13)—O(28)	102.1 (6.0)
O(13)—O(28)—O(19)	89.2 (5.1)
O(28)—O(19)—O(12)	78.6 (3.6)
O(19)—O(12)—O(13)	90.2 (3.7)
O(1)—Me(6)—O(2)	94.3 (3.7)
O(2)—Me(6)—O(23) <sup>2</sup>	98.8 (3.8)
O(23) <sup>2</sup> —Me(6)—O(24) <sup>2</sup>	82.1 (4.0)
O(24) <sup>2</sup> —Me(6)—O(1)	84.9 (3.8)
O(1)—O(2)—O(23) <sup>2</sup>	78.3 (3.4)
O(2)—O(23) <sup>2</sup> —O(24) <sup>2</sup>	97.6 (3.8)
O(23) <sup>2</sup> —O(24) <sup>2</sup> —O(1)	88.9 (4.1)
O(24) <sup>2</sup> —O(1)—O(2)	95.3 (3.7)
O(27)—Me(7)—O(28)	75.6 (3.9)
O(28)—Me(7)—O(29)	98.2 (4.4)
O(29)—Me(7)—O(30)	97.3 (4.4)
O(30)—Me(7)—O(27)	88.9 (4.0)
O(27)—O(28)—O(29)	92.2 (4.4)
O(28)—O(29)—O(30)	91.6 (4.1)
O(29)—O(30)—O(27)	81.5 (3.7)
O(30)—O(27)—O(28)	94.6 (4.4)
O(39)—Me(8)—O(40)	85.0 (3.8)

Table 4 (cont.)

O(40)—Me(8)—O(44)	67.7 (3.8)
O(44)—Me(8)—O(45)	100.3 (3.8)
O(45)—Me(8)—O(39)	106.9 (3.9)
O(39)—O(40)—O(44)	101.4 (4.6)
O(40)—O(44)—O(45)	95.4 (4.2)
O(44)—O(45)—O(39)	79.7 (3.4)
O(45)—O(39)—O(40)	83.4 (3.4)
O(7)—Me(9)—O(8)	84.1 (4.1)
O(8)—Me(9)—O(10)	78.6 (4.6)
O(10)—Me(9)—O(33) <sup>3</sup>	99.3 (4.5)
O(33) <sup>3</sup> —Me(9)—O(7)	97.9 (4.1)
O(7)—O(8)—O(10)	97.9 (4.4)
O(8)—O(10)—O(33) <sup>3</sup>	94.9 (4.7)
O(10)—O(33) <sup>3</sup> —O(7)	82.2 (3.9)
O(33) <sup>3</sup> —O(7)—O(8)	85.1 (3.9)
O(36)—Me(10)—O(37)	80.2 (3.5)
O(37)—Me(10)—O(38)	94.0 (4.4)
O(38)—Me(10)—O(39)	95.9 (4.8)
O(39)—Me(10)—O(36)	89.8 (4.0)
O(36)—O(37)—O(38)	85.2 (3.9)
O(37)—O(38)—O(39)	94.1 (4.2)
O(38)—O(39)—O(36)	92.3 (4.2)
O(39)—O(36)—O(37)	88.4 (3.9)
O(5)—Me(11)—O(6)	91.4 (5.1)
O(6)—Me(11)—O(8)	82.8 (4.2)
O(8)—Me(11)—O(9)	82.4 (3.7)
O(9)—Me(11)—O(5)	103.3 (4.6)
O(5)—O(6)—O(8)	86.3 (4.4)
O(6)—O(8)—O(9)	98.8 (4.2)
O(8)—O(9)—O(5)	71.1 (3.5)
O(9)—O(5)—O(6)	103.7 (4.6)
O(9)—Me(12)—O(13)	68.4 (3.7)
O(13)—Me(12)—O(29)	79.5 (3.3)
O(29)—Me(12)—O(37)	106.1 (4.3)
O(37)—Me(12)—O(9)	106.1 (4.5)
O(9)—O(13)—O(29)	102.1 (4.5)
O(13)—O(19)—O(37)	79.0 (4.0)
O(19)—O(37)—O(9)	84.8 (3.8)
O(37)—O(9)—O(13)	94.1 (3.6)
O(2)—Me(13)—O(3)	102.2 (4.0)
O(3)—Me(13)—O(38)	83.5 (3.9)
O(38)—Me(13)—O(5)	88.9 (3.4)
O(5)—Me(13)—O(2)	85.3 (3.6)
O(2)—O(3)—O(38)	88.9 (4.0)
O(3)—O(38)—O(5)	97.7 (3.9)
O(38)—O(5)—O(2)	79.3 (3.3)
O(5)—O(2)—O(3)	94.0 (3.6)
O(12)—Me(14)—O(10)	72.7 (3.5)
O(10)—Me(14)—O(11)	92.3 (4.1)
O(11)—Me(14)—O(14)	102.9 (4.4)
O(12)—O(10)—O(11)	92.3 (4.3)
O(10)—O(11)—O(14)	93.6 (3.9)
O(11)—O(14)—O(12)	82.1 (3.6)
O(14)—O(12)—O(10)	92.1 (3.8)
O(14)—Me(15)—O(15)	96.2 (4.2)
O(15)—Me(15)—O(18)	97.8 (4.1)
O(18)—Me(15)—O(19)	62.7 (4.2)
O(19)—Me(15)—O(14)	103.2 (4.4)
O(14)—O(15)—O(18)	81.5 (3.7)
O(15)—O(18)—O(19)	98.3 (4.7)
O(18)—O(19)—O(14)	96.9 (4.9)
O(19)—O(14)—O(15)	83.2 (3.7)
O(20)—Me(16)—O(22)	76.9 (3.9)
O(22)—Me(16)—O(26)	87.7 (3.7)
O(26)—Me(16)—O(27)	92.0 (3.8)
O(27)—Me(16)—O(20)	103.3 (4.1)
O(20)—O(22)—O(26)	96.6 (4.4)
O(22)—O(26)—O(27)	86.0 (3.8)
O(26)—O(27)—O(20)	86.7 (3.7)
O(27)—O(20)—O(22)	90.6 (3.9)
O(18)—Me(17)—O(20)	97.3 (4.2)
O(20)—Me(17)—O(21)	77.7 (4.0)

Table 4 (cont.)

O(21)—Me(17)—O(45)	86.2 (3.9)
O(45)—Me(17)—O(18)	98.8 (4.3)
O(18)—O(20)—O(21)	98.4 (4.3)
O(20)—O(21)—O(45)	86.8 (4.0)
O(44)—Me(18)—O(43)	72.8 (4.0)
O(43)—Me(18)—O(15) <sup>2</sup>	92.6 (4.2)
O(16) <sup>2</sup> —Me(18)—O(16) <sup>2</sup>	85.3 (4.3)
O(15) <sup>2</sup> —Me(18)—O(44)	109.3 (4.0)
O(44)—O(43)—O(16) <sup>2</sup>	102.7 (4.7)
O(43)—O(16) <sup>2</sup> —O(15) <sup>2</sup>	86.9 (4.1)
O(16) <sup>2</sup> —O(15) <sup>2</sup> —O(44)	89.6 (4.1)
O(15) <sup>2</sup> —O(44)—O(43)	80.7 (4.0)
O(42)—Me(19)—O(43)	71.6 (4.1)
O(43)—Me(19)—O(17) <sup>1</sup>	82.2 (3.8)
O(17) <sup>1</sup> —Me(19)—O(11) <sup>1</sup>	103.6 (2.8)
O(11) <sup>1</sup> —Me(19)—O(42)	102.6 (4.1)
O(42)—O(43)—O(17) <sup>1</sup>	93.9 (4.2)
O(43)—O(17) <sup>1</sup> —O(11) <sup>1</sup>	89.8 (3.8)
O(17) <sup>1</sup> —O(11) <sup>1</sup> —O(42)	74.9 (3.5)
O(11) <sup>1</sup> —O(42)—O(43)	101.4 (4.5)
O(30)—Me(20)—O(31)	94.4 (4.2)
O(31)—Me(20)—O(34)	94.7 (4.2)
O(34)—Me(20)—O(35)	81.7 (4.3)
O(35)—Me(20)—O(30)	89.2 (4.2)
O(30)—O(31)—O(34)	73.0 (3.6)
O(31)—O(34)—O(35)	105.1 (4.4)
O(34)—O(35)—O(30)	83.7 (4.2)
O(35)—O(30)—O(31)	98.2 (4.0)
O(33)—Me(21)—O(34)	105.9 (3.9)
O(34)—Me(21)—O(41)	93.3 (4.3)
O(41)—Me(21)—O(42)	68.4 (4.1)
O(42)—Me(21)—O(33)	92.4 (3.7)
O(33)—O(34)—O(41)	74.6 (3.4)
O(34)—O(41)—O(42)	115.1 (4.8)
O(41)—O(42)—O(33)	85.2 (4.4)
O(42)—O(33)—O(34)	85.0 (3.4)
O(25)—Me(22)—O(26)	83.2 (4.4)
O(26)—Me(22)—O(31)	105.0 (4.8)
O(31)—Me(22)—O(32)	89.1 (4.6)
O(32)—Me(22)—O(25)	82.6 (4.3)
O(25)—O(26)—O(31)	84.0 (4.4)
O(26)—O(31)—O(32)	93.8 (4.6)
O(31)—O(32)—O(25)	83.5 (4.3)
O(32)—O(25)—O(26)	98.6 (4.9)
O(24)—Me(23)—O(25)	81.0 (4.3)
O(25)—Me(23)—O(4) <sup>1</sup>	90.5 (4.0)
O(4) <sup>1</sup> —Me(23)—O(1) <sup>1</sup>	97.5 (4.3)
O(1) <sup>1</sup> —Me(23)—O(24)	91.0 (4.5)
O(24)—O(25)—O(4) <sup>1</sup>	78.0 (3.6)
O(25)—O(4) <sup>1</sup> —O(1) <sup>1</sup>	92.2 (3.9)
O(4) <sup>1</sup> —O(1) <sup>1</sup> —O(24)	82.9 (4.2)
O(1) <sup>1</sup> —O(24)—O(25)	106.9 (4.8)
O(40)—Me(24)—O(41)	78.8 (3.9)
O(41)—Me(24)—O(42)	66.8 (3.9)
O(42)—Me(24)—O(43)	71.2 (3.9)
O(43)—Me(24)—O(44)	70.2 (3.8)
O(44)—Me(24)—O(40)	72.9 (4.0)
O(40)—O(41)—O(42)	104.7 (5.3)
O(41)—O(42)—O(43)	111.1 (4.9)
O(42)—O(43)—O(44)	107.7 (5.0)
O(43)—O(44)—O(40)	108.7 (5.1)
O(44)—O(40)—O(41)	107.8 (4.7)
O(8)—Me(25)—O(9)	87.6 (3.8)
O(9)—Me(25)—O(13)	62.7 (3.4)
O(13)—Me(25)—O(12)	61.5 (3.3)
O(12)—Me(25)—O(10)	84.0 (3.9)
O(10)—Me(25)—O(8)	64.2 (3.8)
O(8)—O(9)—O(13)	118.1 (4.4)
O(9)—O(13)—O(12)	97.3 (3.6)
O(13)—O(12)—O(10)	122.2 (5.3)
O(12)—O(10)—O(8)	103.4 (4.5)
O(10)—O(8)—O(9)	99.1 (4.6)

Table 4 (cont.)

O(22)—Me(26)—O(23)	73.2 (3.9)
O(23)—Me(26)—O(24)	79.7 (3.8)
O(24)—Me(26)—O(25)	72.9 (3.7)
O(25)—Me(26)—O(26)	57.8 (3.4)
O(26)—Me(26)—O(22)	76.3 (3.6)
O(22)—O(23)—O(24)	109.9 (5.0)
O(23)—O(24)—O(25)	98.3 (4.1)
O(24)—O(25)—O(26)	125.0 (5.1)
O(25)—O(26)—O(22)	97.4 (4.5)
O(26)—O(22)—O(23)	109.4 (4.5)

### Description of the structure

The structure of the compound  $\text{Nb}_8\text{W}_9\text{O}_{47}$  can be described in terms of a ninefold tetragonal tungsten-bronze subcell unit in which twelve of the thirty-six pentagonal rings are completely filled with metal and oxygen atoms. The structure is shown in Fig. 2.

The tetragonal tungsten-bronze subcell unit consists of a continuous host matrix of corner-sharing metal-oxygen octahedra in which the metal atoms are average or (0.4 Nb + 0.6 W) atoms. There are twenty-three crystallographically distinct octahedra of oxygen atoms, each lying in the (001) plane and from which the remaining members are generated according to the symmetry elements of the plane group  $pgg$ . Extension in the [001] direction again occurs by corner sharing. The bond distances and angles listed in Tables 3 and 4 must be used with caution since it has been assumed that all atoms lie in the (001) plane. This is certainly not the actual case and the interatomic distances represent projected or minimum distances. Nevertheless, they satisfactorily depict the packing situation. The metal atoms are displaced from the centres of gravity of their surrounding octahedra of oxygen atoms and in general

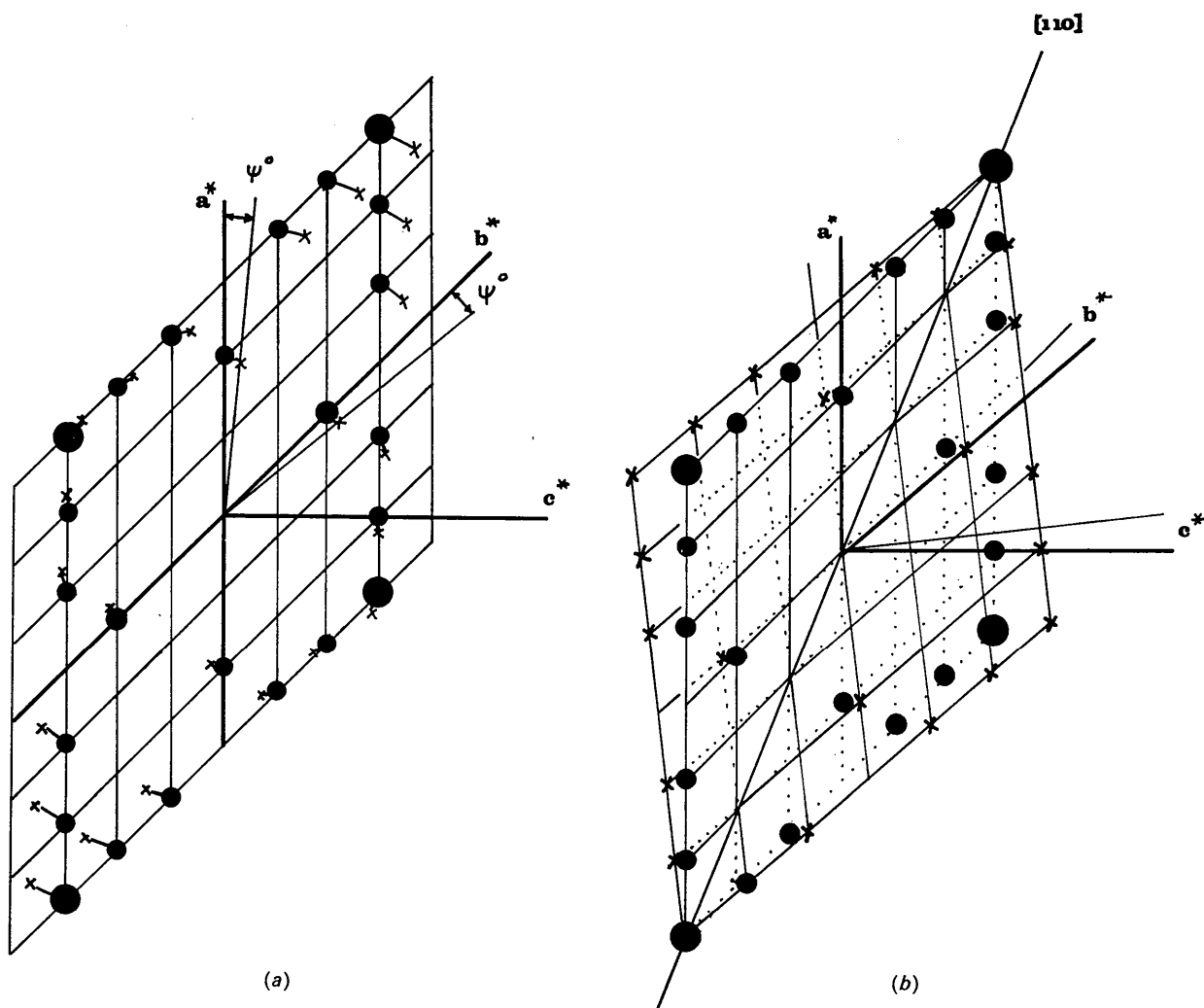


Fig. 3. (a) Sections of the  $hk0$  reciprocal lattice levels of identical crystals which have a common  $c$  axis and have their  $a$  (and  $b$ ) axes inclined by  $\psi^\circ$ . The full circles are associated with crystal 1, whilst the crosses belong to crystal 2. The two reciprocal lattice levels are coplanar. (b) The  $hk0$  reciprocal lattice nets of identical crystals which have a common [110] zone but which are slightly offset with respect to the principal crystallographic axes. The two reciprocal lattice nets are not coplanar.



these displacements are towards adjacent empty square or pentagonal holes. As a result, the empty pentagonal rings are more distorted than those filled with metal and oxygen atoms. The metal–oxygen bond distances compare favourably with those reported for similar structures.

The metal atoms ordered in twelve of the thirty-six pentagonal rings are niobium atoms. These atoms lie in the (001) plane and each is surrounded by five oxygen atoms, approximately in this plane, together with oxygen atoms in apical positions completing a pentagonal bipyramidal polyhedron. These polyhedra share corners and extend infinitely along the [001] direction. The filled pentagonal tunnels are stacked in close-packed hexagonal array parallel to *c*; each tunnel is surrounded by six similar packing tunnels at distances of 9.26–11.75 Å. A similar packing mode is found in the compound  $\text{Nb}_{18}\text{W}_{16}\text{O}_{93}$ .

Each of the filled pentagonal tunnels is surrounded by five square tunnels of corner sharing octahedra and it is interesting that in every instance *one* of these square tunnels contains tungsten or certainly mainly tungsten atoms. Thus *P*(1) adjoins *Me*(4), *P*(2) adjoins *Me*(5)

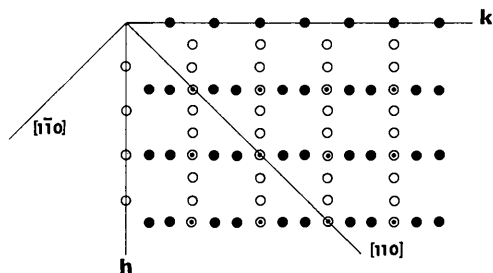


Fig. 4. The  $hk0$  reciprocal lattice level (full circles) of a three-fold tetragonal tungsten-bronze subcell unit. Twinning occurs about the [110] and  $[1\bar{1}0]$  axes and is depicted by the use of open circles. Reflexions with  $h=3n$  and  $k=3n$  overlap, causing vertical splitting of spots to occur on Weissenberg photographs.

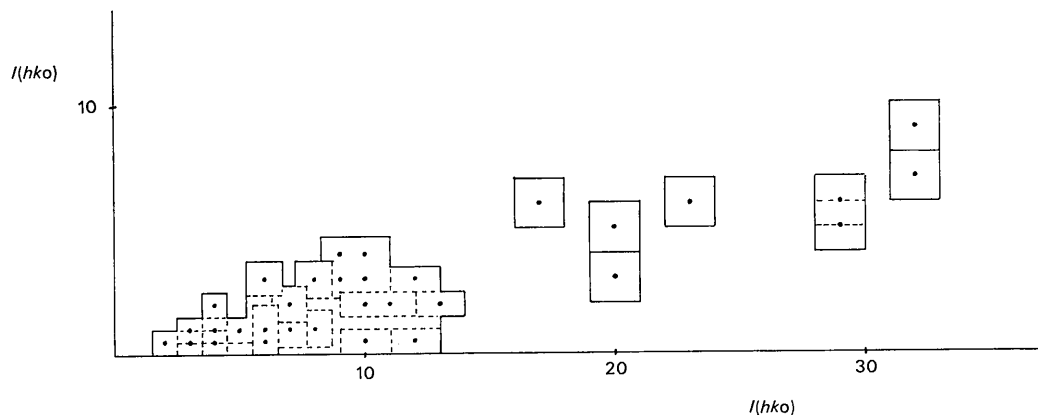


Fig. 5. The orthogonal coordinates of any point on the diagram are proportional to  $I(hk0)$  and  $I(kh0)$ . The rectangle surrounding each point represents reliability limits and, if twinning occurs, it should be possible to draw a straight line passing through the origin and a portion of every rectangle.

and *P*(3) adjoins *Me*(3). The remaining square tunnels contain average atoms.

## Discussion

### Multiple crystals, twinning and intergrowth

An  $hk0$  zero level Weissenberg photograph is practically identical with upper-level equi-inclination Weissenberg photographs and displays the following features:

(1) Reflexions with both  $h=3n$  and  $k=3n$  are much more intense than other reflexions. This is a result of the basic tetragonal tungsten-bronze subcell whose *a* and *b* unit-cell dimensions are approximately one third of the *a* and *b* unit-cell dimensions of the compound  $\text{Nb}_8\text{W}_9\text{O}_{47}$ .

(2) Reflexions with  $h \neq 3n$  are usually less intense than those with  $k \neq 3n$ . This is a result of the manner in which the pentagonal rings are filled – the identity period along the *b* axis direction occurs after three subcell units, whereas along the *a* axis direction an approximate repeat unit occurs after each subcell (see Fig. 2).

(3) All reflexions suffer a horizontal or lateral splitting into two components, indicating the presence of more than one crystal. The most common instance is of two identical crystals aligned with their *c* axes (in this case) parallel to the Weissenberg axis of rotation, and this is shown in Fig. 3(a). If the *a* and *b* axes of each crystal are misoriented by  $\psi^\circ$ , there is a time lag between the passing of any two corresponding reciprocal lattice spots  $h_1k_1l_1$  (crystal 1) and  $h_2k_2l_2$  (crystal 2) through the sphere of reflexion. During this time the camera moves  $\psi/2$  mm and every spot on a Weissenberg photograph is split laterally into two spots separated by  $|\psi/2|$  mm and with intensities depending on the relative volumes of the two crystal components. The weaker spot of each doublet always occurs on the same side of the stronger spot.

The lateral splitting of spots on Weissenberg photographs of the compound  $\text{Nb}_8\text{W}_9\text{O}_{47}$  is slightly different

from that described above. The degree of splitting is not constant on each photograph but increases with  $\theta$ . There is no splitting of 110 type reflexions. Other reflexions are split into weak and strong doublet components; the weaker component is on the left-hand side with doublets on the left-hand side of the [110] axis and on the right-hand side with doublets on the right-hand side of the [110] axis.

The above observations can be explained in terms of two identical crystals with parallel [110] zones and with  $c$  axes slightly inclined to one another [see Fig. 3(b)]. Each member of a doublet is diffracted at the same moment and separation occurs not because of the mechanism of recording, but because points in any one level of the composite reciprocal lattice are not coplanar. A close examination of oscillation photographs showed that each layer of spots was actually split into two layers, one being much more intense than the other. It is estimated, from a measurement of the angular separation of the two 420 reflexions that the  $c$  axes of the two identical crystals comprising the whole are inclined at an angle of  $1^\circ 24'$ .

(4) At Bragg angles greater than about  $50^\circ$  spots with both  $h=3n$  and  $k=3n$  are split vertically; actually, triplets occur owing to  $\alpha_1\alpha_2$  overlap. This is caused either by twinning or by the intergrowth of another phase which has a crystal structure similar to that of Nb<sub>8</sub>W<sub>9</sub>O<sub>47</sub>. This phase would be expected to be Nb<sub>6</sub>W<sub>8</sub>O<sub>39</sub>, which is described by Roth (1967) as tetragonal with  $a=12.190$  and  $c=3.968$  Å.

Twinning would occur about the [110] and [1 $\bar{1}$ 0] axes so that, for example  $h00$  reflexions from one twin fall

on the  $0k0$  reflexions from the other. Because of the small differences between  $a$  and  $b$  cell dimensions the overlap is not exact and splitting occurs along the [ $h00$ ] and [ $0k0$ ] festoons. However, one would expect, from this hypothesis, that *all* reflexions other than  $hh0$  type would show vertical splitting, but this is not so. This difficulty can be overcome by choosing a unit cell for the compound Nb<sub>8</sub>W<sub>9</sub>O<sub>47</sub> which is based upon three tetragonal tungsten bronze subcells and has dimensions  $a=12.23$ ,  $b=36.57$  and  $c=3.945$  Å. In this case twinning occurs about the [130] and [1 $\bar{3}$ 0] axes of this new cell and under these conditions:

(a) Reflexions with both  $h=3n$  and  $k=3n$  (original indexing based upon the larger cell) will be split vertically.

(b) Reflexions with either  $h=3n$  or  $k=3n$  will not be split.

(c) No reflexions will occur when both  $h \neq 3n$  and  $k \neq 3n$ .

This situation is depicted in Fig. 4 and does, in fact, describe the observations well. A 200 hr zero level Weissenberg exposure failed to reveal any reflexions in category (c). The fact that  $hk0$  reflexions with  $h \neq 3n$  are usually much less intense than  $hk0$  reflexions with  $k \neq 3n$  is now explained in terms of a low twin ratio, since the former type of reflexions is related to the latter by twinning. A problem has thus arisen which can be reframed in the following manner:

(a) The unit-cell of Nb<sub>8</sub>W<sub>9</sub>O<sub>47</sub> has a structure based upon ninefold tetragonal tungsten-bronze subcells and vertical splitting of some reflexions arises from the intergrowth of another phase, *i.e.* Nb<sub>6</sub>W<sub>8</sub>O<sub>39</sub>; or

Table 5. Atomic parameters for Nb<sub>8</sub>W<sub>9</sub>O<sub>47</sub> based upon a threefold tetragonal tungsten-bronze subcell unit

Standard deviations and atomic symbols are as denoted in Table 1. Oxygen atoms (not listed) are to be superimposed on Me and P atoms, each with a  $z/c$  coordinate of 0.50. Each oxygen atom has a thermal parameter  $B=2.0$  Å<sup>2</sup>.

The effective atomic numbers are: Nb=40.4, W=68.0 and (0.4Nb+0.6W)=57.0.

	$x/a$	$y/b$	$B$	Effective $z$
Me(1)	0.00000	0.50000	1.47 (31) Å <sup>2</sup>	57.9 (4.7)
Me(2)	0.07449 (67)	0.07020 (16)	1.85 (23)	55.9 (4.5)
Me(3)	0.07064 (59)	0.40281 (14)	1.66 (22)	59.3 (4.6)
Me(4)	0.42126 (73)	0.23253 (16)	1.88 (25)	56.2 (4.6)
Me(5)	0.29577 (68)	0.47828 (15)	1.59 (19)	58.7 (4.4)
Me(6)	0.21066 (60)	0.30714 (14)	1.56 (19)	59.1 (4.5)
Me(7)	0.29472 (66)	0.13871 (15)	1.87 (21)	57.4 (4.5)
Me(8)	0.01446 (55)	0.17326 (13)	1.78 (20)	67.2 (5.2)
P(1)	0.33346 (82)	0.38965 (21)	2.09 (29)	44.2 (3.8)
O(1)	0.3451 (64)	0.0023 (18)		
O(2)	0.1121 (69)	0.0215 (18)		
O(3)	0.2142 (70)	0.0933 (18)		
O(4)	0.4480 (66)	0.1220 (20)		
O(5)	-0.0021 (71)	0.4495 (18)		
O(6)	0.1386 (71)	0.1662 (17)		
O(7)	-0.0006 (76)	0.2238 (19)		
O(8)	0.0578 (70)	0.2908 (18)		
O(9)	0.2833 (76)	0.2612 (18)		
O(10)	0.3551 (69)	0.1890 (17)		
O(11)	0.3662 (74)	0.3372 (17)		
O(12)	0.1905 (69)	0.3614 (18)		
O(13)	0.1951 (71)	0.4281 (19)		
O(14)	0.4019 (66)	0.4413 (19)		
O(15)	-0.0008 (67)	0.0026 (21)		

(b) The unit cell of  $\text{Nb}_8\text{W}_9\text{O}_{47}$  has a structure based upon threefold tetragonal tungsten-bronze subcells and twinning causes splitting of some reflexions where overlap occurs.

If this latter case offers the correct description of the structure, then the question also arises, does the structure of the untwinned unit cell of  $\text{Nb}_8\text{W}_9\text{O}_{47}$  basically differ from that described above for it on the basis ninefold tetragonal tungsten-bronze subcells?

In theory the following method can be used in an attempt to distinguish between the two cases. If case (b) prevails, then reflexions for which  $h \neq 3n$  and  $k \neq 3n$  have arisen because of twinning. A typical reflexion  $hk0$  will be generated from  $hk0$  and  $kh0$  planes and, because the twin ratios are constant for a particular crystal, the ratio  $F_{\text{obs}}^2(hk0)/F_{\text{obs}}^2(kh0)$  will be constant for reflexions with  $h \neq 3n$  and  $k = 3n$ . A rigid statistical analysis of these ratios to determine whether or not they are constant within the limits of error of the observed data is complicated by the fact that the exact values of  $F_{\text{obs}}^2(hk0)$  are not known. Only crude estimates are known, based upon a comparison with intensities recorded on a calibrated strip. It is doubtful whether a number of estimations of the intensity of any one reflexion by this comparison method will give a true value for  $F_{\text{obs}}^2(hkl)$  together with a statistically acceptable standard error. However, the following approach can be made. Fig. 5 shows a plot of points whose orthogonal coordinates are proportional to estimates for  $F_{\text{obs}}^2(hk0)$  and  $F_{\text{obs}}^2(kh0)$ . Within the limits of the errors of observation these points should lie in a straight line passing through the origin if twinning occurs. The estimated errors in the actual observations are depen-

dent on the magnitude of the observation (*viz.*  $2 \pm 1$ ,  $10 \pm 1$ ,  $20 \pm 2$ ,  $30 \pm 3$ ) and a rectangle can be dotted around each spot to indicate reliability limits. It is apparent that *no* straight line can be drawn so that it passes through a portion of every rectangle. This in itself cannot be taken as reliable statistical evidence although it does tend to support the view that the structure of  $\text{Nb}_8\text{W}_9\text{O}_{47}$  is correctly based upon a ninefold tetragonal-bronze subcell unit.

*The structure of  $\text{Nb}_8\text{W}_9\text{O}_{47}$  described in terms of a threefold tetragonal tungsten-bronze subcell unit*

If  $hk0$  reflexions with  $h \neq 3n$  and  $k = 3n$  are considered to arise from twinning they may be ignored and the remaining reflexions reindexed on the basis of a unit cell with dimensions  $a = 12.23$ ,  $b = 36.57$  and  $c = 3.945$  Å. Those remaining reflexions do not represent the contribution from one twin: reflexions with  $k \neq 3n$  will arise from one twin alone but reflexions with  $k = 3n$  will be overlapping reflexions from both twins. The Fourier coefficients arising from reflexions of the latter type will be of the form  $[(1 + \lambda)F^2(hk0)]^{1/2}$ , where  $\lambda$  is the twin ratio and these terms will contribute mainly to atoms associated with the tetragonal tungsten-bronze subcell in the resulting electron density map, *i.e.* metal and oxygen atoms associated with octahedral coordination polyhedra.

The twin ratio,  $\lambda$ , was determined by a least-squares procedure in which  $\sum |F^2(hk0) - \lambda F^2(kh0)|^2$  was minimized. The data used involved reflexions with either  $h = 3n$  or  $k = 3n$  (original indexing based upon the larger unit cell) and the value of  $\lambda$  proved to be 0.20. The overall effect of using the data described above is merely to increase the electron density associated with any atoms of the basic subcell units by 10% above what it would be were data from one twin only to have been used.

The relevant  $hk0$  reflexions were therefore reindexed on the basis of the smaller unit cell and the ideal atomic coordinates of atoms comprising the asymmetric unit were calculated as before. The space group, determined from systematic absences in spectra, remains  $P2_12_12$  and this has some interesting consequences. For instance, metal atoms Me(3), Me(4) and Me(5) of Table 1 were previously unrelated by the symmetry elements associated with the ninefold tetragonal tungsten-bronze subcell unit. However, these atoms and those related to them by the symmetry elements of the larger unit cell (12 atoms in all) are now, each and every one, related to one another by the symmetry elements and unit-cell translations associated with the smaller threefold tetragonal tungsten-bronze subcell units. There is a greater restriction placed upon the number of variables associated with atoms listed in Table 1, and this is in accordance with the smaller number of reflexions made available as a result of reindexing. However, because of the different locations of the symmetry elements and the resultant differing locations of the symmetry elements and the resultant differing atoms related by them, it is possible that a different structure will result when

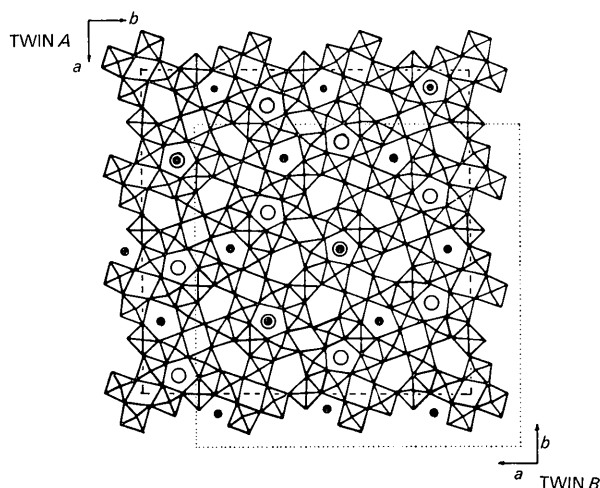


Fig. 6. An [001] projection of the twinned  $\text{Nb}_8\text{W}_9\text{O}_{47}$  structure. Open circles represent the tunnels of Me and oxygen atoms which belong to twin A, whilst full circles represent the similar tunnels of twin B. The twins are stacked, ABAB etc. in a direction parallel to c. The diagram shows that the tunnels of adjacent domains pack according to a hexagonal close packed array in that each open circle is surrounded by three full circles.

the threefold tetragonal tungsten-bronze subcell unit is refined; not so much as in a different positioning of atoms, but rather in a different pattern of atomic ordering as evidenced by a different distribution of occupancy factors.

The structure solution and refinement was carried out in a manner similar to that described above for the ninefold tetragonal tungsten-bronze subcell unit. The final atomic coordinates are listed in Table 5.

#### Discussion of the threefold tetragonal tungsten-bronze subcell structure

The meaningful temperature parameters for the metal atoms and the low value for the residual ( $R=0.07$ ) are factors in favour of describing the structure of Nb<sub>8</sub>W<sub>9</sub>O<sub>47</sub> in terms of threefold tetragonal tungsten-bronze subcells. However, the overall picture remains the same as that reported above; the octahedrally coordinated metal atoms are essentially average atoms ( $0.4 \text{ Nb} \pm 0.6 \text{ W}$ ) whilst the metal atoms associated with pentagonal bipyramidal polyhedra are niobium, or mainly niobium atoms. The metal atom Me(8) in Table 5, corresponding to metal atoms Me(3), Me(4) and Me(5) in Table 1, is either a tungsten atom, or certainly more likely to be tungsten rather than niobium and these atoms prefer positions adjacent to niobium-rich polyhedra. Areas of accumulated electrical charge are therefore minimized.

Although the refinement of the structure of Nb<sub>8</sub>W<sub>9</sub>O<sub>47</sub> in terms of threefold tetragonal tungsten-bronze subcells does not produce any change in the ordering or distribution of atoms in three dimensions, it is of interest to determine whether the reduction in the number of reflexions and in the number of parameters available to describe the positions of these atoms does in effect produce any significant changes in the structure itself. Table 6 gives the parameters of the crystallographically independent metal atoms of Table 1 as calculated from appropriate parameters listed in Table 5. The differences in the respective coordinates calculated on the basis of ninefold and threefold tetragonal tungsten-bronze subcell units are also given. In some cases these differences are significant and in all cases they are small, of the order of 0.04 Å. On the basis of the standard deviations in atomic positions listed in Tables 1 and 5, a difference in  $x$  coordinates of 0.0012 and in  $y$  coordinates of 0.0011, is significant at the 0.1% level.

Table 6. Fractional atomic coordinates for the crystallographically independent atoms of a ninefold tetragonal tungsten-bronze subcell unit as calculated from the atomic parameters of Table 5

The columns headed  $\Delta x/a$  and  $\Delta y/b$  give the differences between coordinates listed in this Table and the corresponding coordinates listed in Table 1.

	$x/a$	$y/b$	$\Delta x/a$	$\Delta y/b$
Me(1)	0.00000	0.50000	0	0
Me(2)	0.16667	0.00000	0.00086	0.00124

Table 6 (cont.)

	$x/a$	$y/b$	$\Delta x/a$	$\Delta y/b$
Me(3)	0.00482	0.17326	0.00034	0.00124
Me(4)	0.17148	0.32674	0.00003	0.00156
Me(5)	0.33815	0.17326	0.00050	0.00191
Me(6)	0.02483	0.07020	0.00076	0.00033
Me(7)	0.30708	0.26747	0.00190	0.00110
Me(8)	0.07022	0.30714	0.00066	0.00087
Me(9)	0.26525	0.02172	0.00064	0.00036
Me(10)	0.14042	0.23253	0.00112	0.00008
Me(11)	0.19024	0.09719	0.00310	0.00034
Me(12)	0.23688	0.19286	0.00133	0.00060
Me(13)	0.09824	0.13871	0.00163	0.00244
Me(14)	0.35816	0.07020	0.00055	0.00119
Me(15)	0.43157	0.13871	0.00011	0.00042
Me(16)	0.40355	0.30714	0.00007	0.00207
Me(17)	0.47375	0.23253	0.00105	0.00040
Me(18)	0.02358	0.40281	0.00091	0.00029
Me(19)	0.09859	0.47828	0.00109	0.00058
Me(20)	0.26490	0.36129	0.00100	0.00008
Me(21)	0.19149	0.42980	0.00072	0.00140
Me(22)	0.35691	0.40281	0.00114	0.00061
Me(23)	0.43192	0.47828	0.00037	0.00061
P(1)	0.11115	0.38965	0.00153	0.00117
P(2)	0.27781	0.11035	0.00174	0.00172
P(3)	0.44448	0.38965	0.00295	0.00003

Apart from small differences in atomic positions (and therefore, in bond distances and angles) the description of the structure of the compound Nb<sub>8</sub>W<sub>9</sub>O<sub>47</sub> is essentially the same whether it is based upon a threefold or ninefold tetragonal tungsten-bronze subcell unit. However, the question still remains as to whether the vertical splitting of some reflexions is the result of twinning or of the intergrowth of a structurally similar phase, namely Nb<sub>6</sub>W<sub>8</sub>O<sub>39</sub>.

It has been shown above that certain of the five-sided tunnels, which extend infinitely in a direction parallel to the  $c$  axis of the tetragonal tungsten-bronze type structure, are completely filled with mainly niobium atoms and oxygen atoms and that these niobium atoms are in pentagonal bipyramidal coordination. These filled pentagonal tunnels are distributed throughout the structure in a close-packed hexagonal array. If this structure is rotated through 180° about the [110] axis (indexed on the basis of a ninefold subcell unit) then these two structures are related as the twins described above. A subsequent translation of the origin of one twin by approximately  $a/4 + b/4$  causes the host lattice of corner-sharing octahedra of each twin to become superimposable or interpenetrable. However, in 83% of these cases the filled pentagonal tunnels do not superimpose; the filled pentagonal tunnels of twin *B* stack above empty tunnels of twin *A* in the same way that layers of metal atoms stack together in a hexagonal close-packed metal structure, *i.e.* *ABAB* etc. (see Fig. 6). A reason for twinning thus becomes apparent – it provides a mechanism by which the symmetrically distributed filled pentagonal tunnels may become more evenly distributed in a continuous host matrix of corner-sharing octahedra.

On the other hand, if the supposed intergrowth phase Nb<sub>6</sub>W<sub>8</sub>O<sub>39</sub> is to have a structure similar to that of Nb<sub>8</sub>W<sub>9</sub>O<sub>47</sub>, *i.e.* a ninefold tetragonal tungsten-bronze subcell unit, the compositional parallelogram would

require 18 *half-filled* pentagonal tunnels per unit cell and this very closely resembles the twinned structure depicted in Fig. 6. Provided the molar ratio is 1:1, the difference between these two structures is that  $\frac{1}{6}$  of the 18 pentagonal tunnels in the twinned  $\text{Nb}_8\text{W}_9\text{O}_{47}$  structure are *completely* filled. This is not unexpected since the difference between metal: oxygen ratios in the two compounds  $\text{Nb}_8\text{W}_9\text{O}_{47}$  and  $\text{Nb}_6\text{W}_8\text{O}_{39}$  is less than 1%.

The structure of a crystal of the compound  $\text{Nb}_8\text{W}_9\text{O}_{47}$  can thus be described in terms of the ninefold tetragonal tungsten-bronze subcell unit outlined above together with an intergrowth phase of probable composition  $\text{Nb}_6\text{W}_8\text{O}_{39}$ . Alternatively, a similar description involves a threefold tetragonal tungsten-bronze subcell unit which is twinned about the [130] axis. It is probable that both twinning and intergrowth of phases occur in the one crystal.

#### References

- ANDERSSON, S. (1965). *Acta Chem. Scand.* **19**, 2285.  
 BUSING, W. R., MARTIN, K. O. & LEVY, H. A. (1962). *ORFLS. A Fortran Crystallographic Least-Squares Program*. USAEC Report ORNL-TM-305.  
 BUSING, W. R., MARTIN, K. O. & LEVY, H. A. (1964). *ORFFE. A Fortran Crystallographic Function and Error Program*. USAEC Report ORNL-TM-306.  
 CRUICKSHANK, D. W. J. (1965). *Computing Methods in Crystallography*. Ed. J. S. ROLLETT. Oxford: Pergamon Press.  
 DAUBEN, C. H. & TEMPLETON, D. H. (1955). *Acta Cryst.* **8**, 841.  
 HÄGG, G. & MAGNÉLI, A. (1954). *Rev. Pure Appl. Chem.* **4**, 235.  
 HOERNI, J. A. & IBERS, J. A. (1954). *Acta Cryst.* **7**, 744.  
 KIHLBORG, L. (1963). *Acta Chem. Scand.* **17**, 1485.  
 MAGNÉLI, A. (1949). *Ark. Kemi*, **1**, 213.  
 ROTH, R. S. (1967). Private communication.  
 ROTH, R. S. & WADSLEY, A. D. (1965). *Acta Cryst.* **19**, 26.  
 RUBIN, J. J., UITERT, L. G. VAN & LEVINSTEIN, H. J. (1968). *Int. J. Cryst. Growth*, In the press.  
 SLEIGHT, A. (1966). *Acta Chem. Scand.* **20**, 1102.  
 SLEIGHT, A. & MAGNÉLI, A. (1964). *Acta Chem. Scand.* **18**, 2007.  
 STEPHENSON, N. C. (1965). *Acta Cryst.* **18**, 496.  
 STEPHENSON, N. C. (1968). *Acta Cryst.* **B24**, 637.  
 THOMAS, L. H. & UMEDA, K. (1957). *J. Chem. Phys.* **26**, 293.

*Acta Cryst.* (1969). **B25**, 2083

## The Crystal and Molecular Structure of Cyclopropanecarboxamide\*

BY ROBERT E. LONG,† HANNELORE MADDOX AND KENNETH N. TRUEBLOOD

*Department of Chemistry,‡ University of California, Los Angeles, California 90024, U.S.A.*

(Received 2 December 1968)

Cyclopropanecarboxamide,  $\text{C}_4\text{H}_7\text{NO}$ , crystallizes in space group  $P2_1/c$ , with  $a_0=6.919$ ,  $b_0=8.271$ ,  $c_0=16.313$  Å,  $\beta=90.22^\circ$ , and two molecules in the asymmetric unit. The structure was solved by direct methods and was refined by full-matrix least-squares, with visually estimated three-dimensional photographic intensity data. The two independent molecules have essentially the same dimensions and conformation, which are comparable with those for related compounds. Hydrogen bonds link the molecules three-dimensionally, each molecule being involved in four such bonds. The two molecules show nearly identical librational patterns, the predominant motion for each being a  $9.6^\circ$  libration about an axis close to the molecular axis of minimum inertia.

### Introduction

This investigation was begun in 1954 but, for various reasons, was not completed until recently. The original purpose was to provide precise structural data on a three-membered ring compound. Although no such

structural studies of crystalline compounds had then been reported, several precise determinations have since appeared, together with several careful electron diffraction and microwave analyses. The most precise of the crystallographic studies (Fritchie, 1966; Hartman & Hirshfeld, 1966) have even provided evidence to support the bent-bond model for the three-membered ring (Coulson & Moffitt, 1949; Coulson & Goodwin, 1962). The present study, based on visually estimated photographic data is not accurate enough for that, but does provide reasonably precise molecular dimensions, further data on the hydrogen-bonding schemes of amides, and information of interest in

\* Supported in part by the U.S. Air Force Office of Scientific Research, Contract AF49(638)-719 and Grant AF-AFOSR-240-63 and by the National Science Foundation, Grant GB-2029.

† Present address: System Development Corporation, 2500 Colorado Blvd., Santa Monica, California 90406.

‡ Contribution No. 2299.